Hybrid Cathode Materials

DOI: 10.1002/ange.201200210

Redox-Active Metal-Centered Oxalato Phosphate Open Framework Cathode Materials for Lithium Ion Batteries**

Mangayarkarasi Nagarathinam, Kuppan Saravanan, Eunice Jia Han Phua, M. V. Reddy, B. V. R. Chowdari, and Jagadese J. Vittal**

Dedicated to Professor Phil Dean on the occasion of his birthday

Discovering revolutionary cathode materials for lithium ion batteries (LIBs) with a high power/energy density to confront the existing energy, economic, and ecologic crises is one of the persistent challenges in materials research.[1] The most promising olivine phosphate $LiMPO_4$ electrode materials (M = Fe, Mn, or Co)[2] have already attained maximum capacity through the development of new synthetic methods, such as downsizing,[3] conductive wiring,[3b,4] and doping.[5] Recently, hierarchical olivine-based materials produced by soft synthetic strategies have been shown to have higher bulk density, superior performance at high rates, and better cycling stability.[6] Besides commercialization of olivine phosphates, current research is also focused on enhancing the performance of LIBs for high-current applications by developing new electrode materials. Many alternative candidates, such as $Li_3M_2(PO_4)_3$,[7] Li_2MSiO_4,[8] $LiMSO_4F$,[9] $LiMBO_3$[1d,10] (M = Fe, V, Mn, Co, etc.) $LiVOPO_4$,[11] $LiVPO_4F$,[12] and $Li_2FeP_2O_7$[13] have been pursued as cathode materials.

Further to these inorganic materials, new organic[14] and metal–organic framework[15] (MOF) materials have also shown promise as electrode materials for LIBs. The major challenges ahead in the utilization of MOFs as electrode materials for LIBs are the high molecular weight, low density, difficulty of synthesizing large quantities, and challenging isolation of robust MOFs with redox-active metal centers, compared to inorganic materials.[15a,c] These drawbacks may delay their utilization and commercialization as cathode materials.

For this reason, it is worthwhile to investigate energy storage in an entirely new class of phosphate-based hybrid materials.[16] Metal organic–phosphate open frameworks (MOPOF) are hybrid materials with multidimensional architectures constructed from transition-metal phosphates cross-linked by simple organic linkers, which in turn can encapsulate a diverse range of alkali ions (Li^+, Na^+, and K^+) between the layers.

Though MOPOFs are well known for their structural diversity and for conventional industrial applications, such as redox reactions, catalysis, gas storage, and MRI contrast agents, these materials have not been investigated as energy storage materials.[17] The presence of mixed organic oxalate and inorganic phosphate anions is expected to enhance the redox properties of the transition-metal ions, provide robustness to the material, and reduce the synthesis temperature required, along with the versatility offered by the organic ligands. Furthermore, the synthetic simplicity of MOPOFs with redox-active metal centers and the possible two-dimensional migration pathways for M^+ ions (deduced from careful analysis of the packing patterns of the reported crystal structures) motivated us to investigate these MOPOFs as cathode materials for LIBs. Herein, we disclose for the first time the lithium storage performance of MOPOFs $K_{2.5}[(VO)_2(HPO_4)_{1.5}(PO_4)_{0.5}(C_2O_4)]$, **1**, $Na_2[(VO)_2(HPO_4)_2(C_2O_4)]$, **2**, and the $KLi[(VO)_2(HPO_4)_2(C_2O_4)]$, **3**.

Hydrothermal treatment of an aqueous solution of H_3PO_4, V_2O_5, and $K_2C_2O_4$ at 120 °C resulted in bluish-green plates of **1** (See Supporting Information, Figure S1). The single-crystal X-ray structure of **1** reveals that the asymmetric unit is composed of one formula unit $K_{2.5}[(VO)_2(HPO_4)_{1.5}(PO_4)_{0.5}(C_2O_4)]\cdot 4.5\,H_2O$. The V^{IV} atom has a distorted VO_6 octahedral core comprised of O atoms from three different HPO_4^{2-} and PO_4^{3-} groups, two O atoms from a chelating oxalato $(C_2O_4)^{2-}$ anion, and one oxo ligand with a short V=O bond (1.59 Å). Three vanadium octahedra are corner-shared by tetrahedral HPO_4^{2-}/PO_4^{3-} anions and vice versa to form infinite chains of $[(VO)(HPO_4)_{1.5}(PO_4)_{0.5}]$ (see Supporting Information, Figure S2). The vanadium atoms in the adjacent chains are connected by bridging $C_2O_4^{2-}$ anions and thus results in an anionic layer of $[(VO)_2(HPO_4)_{1.5}(PO_4)_{0.5}(C_2O_4)]^{2.5-}$ in the *ab* plane, as shown in Figure 1. The two-dimensional layers are interleaved by K^+ ions and H_2O molecules (see Supporting Information, Figure S3). The oxidation state of vanadium as V^{IV} is supported by the

[*] Dr. M. Nagarathinam, Dr. K. Saravanan, E. J. H. Phua, Prof. J. J. Vittal
Department of Chemistry, National University of Singapore
Singapore 117543 (Singapore)
E-mail: chmjjv@nus.edu.sg
Dr. M. V. Reddy, Prof. B. V. R. Chowdari
Department of Physics, National University of Singapore
Singapore 117543 (Singapore)
E-mail: phymvvr@nus.edu.sg
Prof. J. J. Vittal
Department of Chemistry, Gyeongsang National University
Jinju (South Korea)

[**] We thank the Ministry of Education, Singapore for funding (R-143-000-484-112), H. K. Wong, Department of Physics, NUS for recording XPS data, and Prof. G. V. Subba Rao and A. Shahul Hameed for the constant support and encouragement. J.J.V. thanks the Ministry of Education, Science & Technology (S. Korea) for the World Class University Chair Professorship through the Grant No. R32-2008-000-2003-0.

Supporting information for this article is available on the WWW under http://dx.doi.org/10.1002/anie.201200210.

© 2012 Wiley-VCH Verlag GmbH & Co. KGaA, Weinheim

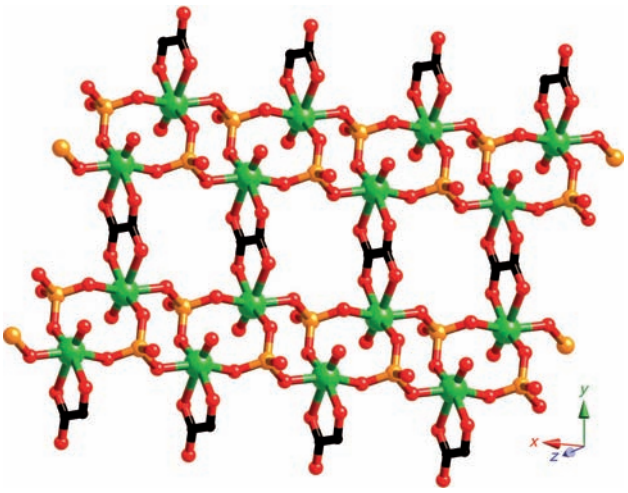

Figure 1. A perspective view of the layered structure of **1** (H and K atoms are omitted for clarity). V green, P orange, O red, C black.

presence of 2.5 crystallographically different K^+ ions, and the charge is balanced by 1.5 HPO_4 and 0.5 PO_4 anions.

The bond-valence calculation of the V atoms of **1** shows the presence of only V^{IV} (IV oxidation state = 4.07 and 4.09) and supports the assigned molecular formula $K_{2.5}[(V^{IV}O)_2(HPO_4)_{1.5}(PO_4)_{0.5}(C_2O_4)]\cdot 4.5\,H_2O$.[18] X-ray photo-electron spectroscopy (XPS) studies further confirmed the oxidation state of vanadium atoms as V^{IV}, and the characteristic binding energies of V, K, P, and O elements are presented in Supporting information, Figure S4.

The K1 and K2 cations located in the interlayer space possess facile two-dimensional migration pathways in the *ab* plane (Figure 2). Interestingly, the existence of channels along the *c* axis favors the migration of K^+ ions in the third dimension also (see Supporting Information, Figure S3). On the other hand, these channels may further assist the diffusion of alkali ions/Li^+ ions in the *c* direction (which is occupied by aqua ligands) and promote the subsequent extraction of K^+ ions in the *ab* plane. The prevailing robustness of the anion shows that it is possible to substitute K^+ with Li^+ ions and that these materials are appropriate for continuous extraction and insertion of Li^+ ions when compared to the available $LiFePO_4$ with a one-dimentional migration pathway.[19] The crystal density of the MOPOF material **1** is 2.425 $g\,cm^{-3}$, which outweighs the density of the reported MOFs (MIL-53Fe 1.7 $g\,cm^{-3}$)[15a] and the developing organic[14a,b] electrode materials. A sodium analogue $Na_2[(V^{IV}O)_2(HPO_4)_2(C_2O_4)]\cdot 2\,H_2O$ (**2**) with two environmentally different Na atoms has also been synthesized by a modified procedure and characterized (Supporting Information, Figure S5).[20]

Thermogravimetric analysis (TG) of **1** showed two-step weight loss in the range 30–90 °C (5 %) and 90–110 °C (7 %), owing to the complete removal of uncoordinated and coordinated water molecules, respectively, in the crystal. The compound **1** is thermally stable up to 300 °C and oxalate ligand is removed at 300–350 °C (weight loss of 14 % shown in Supporting Information, Figure S6).

The powder X-ray diffraction pattern (PXRD) of **1** after dehydration, followed by ball milling with Super P carbon for 4 h, matched with the parent crystals. The lattice parameters $a = 6.366$ Å, $b = 9.131$ Å, and $c = 14.620$ Å of the dehydrated material, obtained from the Rietveld refinement (using TOPAS R 2.1 software), were close to those of **1**. This result confirms that the removal of water and reduction of the crystal size can be carried out without sacrificing the phase of the crystal structure (see Supporting Information, Figure S7). The galvanostatic charge–discharge profiles and capacity versus cycle number plots (Figure 3 inset) of **1** are shown in Figure 3, at a current density of 40 $mA\,g^{-1}$ (0.30 C) within the voltage window of 2.5–4.6 V.

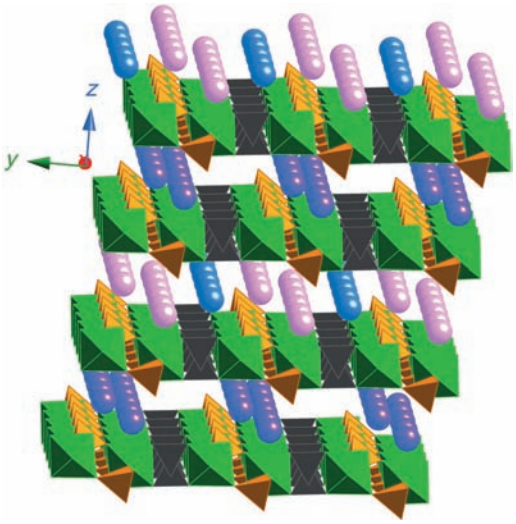

Figure 2. Packing pattern of **1** viewed along the *a* axis. Green VO_6 octahedra, orange PO_4 tetrahedra, black oxalato C atoms, purple K1, pink K2, blue K3. Hydrogen atoms are omitted for clarity.

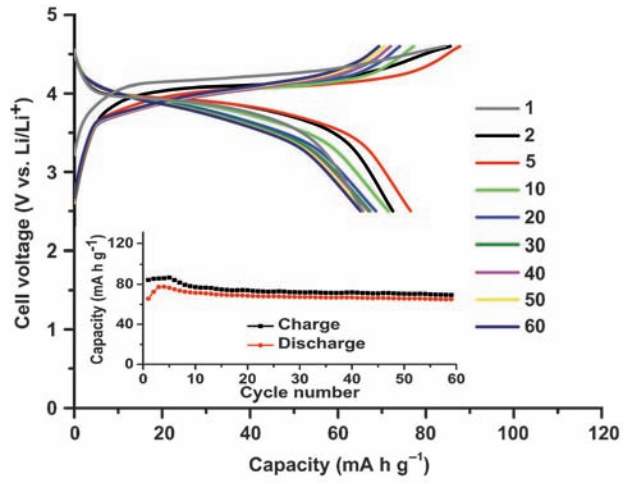

Figure 3. Galvanostatic charge–discharge profiles (at cycles given) and cyclability (inset) of dehydrated crystals of **1** at a current density of 40 $mA\,g^{-1}$ (0.30 C, where 1C = 108 $mA\,g^{-1}$) in the voltage range of 2.5–4.6 V. Theoretical specific capacity of **1** upon complete removal of 2 K^+ ions is 108 $mA\,h\,g^{-1}$, from the structure.

© 2012 Wiley-VCH Verlag GmbH & Co. KGaA, Weinheim

The first charge cycle shows a single flat plateau at 4.16 V, which corresponds to the extraction of K^+ ions and resulted in a charge capacity of 85 mA h g^{-1}. Subsequent discharge (re-insertion of Li^+ ions into the **1** structure) occurs at 4.0 V, with the reversible capacity of 66 mA h g^{-1}, corresponds to the one-electron theoretical capacity.

It is believed that K^+ ions are extracted from the framework upon charging. Generally, mixed Li/K intercalation/deintercalation is expected from the first discharge cycle and subsequent cycles. But with the increase in the ionic mobility with respect to the decrease in ionic radius (*r*Li: 0.76 Å, *r*K: 1.38 Å), the Li^+-ion-rich cell is expected to favor the passage of Li^+ ions in the subsequent charge and discharge cycles, rather than the heavier K^+ ion through the electrode.[12a,21] To understand the electrode kinetics, electrochemical impedance spectroscopy (EIS) studies were carried out on electrodes made of **1**. The comparative Nyquist plots (Z' and $-Z''$) of the cell during the first and fifth cycles in the charged state are shown in the Supporting Information Figure S8 and the fitted impedance values are summarized in Table S1. The preliminary EIS results reveal that the overall increase in impedance occurs as a result of the change in voltage during the first charge cycle, which clearly indicates the de-intercalation of K^+ ion from the host lattice. The slight or marginal decrease of the overall impedance of the same cell after the fifth cycle in the charged state (4.6 V) in comparison to the results of first cycle further supports the exchange of Li^+ ions during discharge and the subsequent structural modification during cycling. The improvement in the Warburg lines (inclination) at low-frequency region of the spectra (see Supporting Information, Figure S8b) strongly suggests that the Li^+ ion diffusion conditions were improved upon cycling (after the fifth cycle) because of the removal of K^+ ions.[22] The ex situ energy dispersive X-ray spectrum (EDX) of the cycled electrode charged at 4.6 V, after careful dismantling in the glove box, shows a decrease in the K/V or K/P ratio to 0.45 compared to the ratio (K/V = 1) in the bare electrode. This further confirms the removal of K^+ ions in the first cycle (see Supporting Information, Figure S9).

Further, the galvanostatic charge–discharge profiles show that the successive lithium extraction occurs at slightly lower voltage (3.98 V) than the first cycle (4.0 V). The redox potential values are higher than $LiFePO_4$ (3.5 V versus Li) and similar to $LiVOPO_4$[11b] and $LiVPO_4F$.[12b] The small hysteresis (ΔV) of 0.16 V (ΔV = voltage difference between the charge and discharge curves) is indicative of the favorable energetic reversibility of the alkali ion insertion/extraction in **1**. Even though coulombic efficiencies of the first few cycles are found to be poor, significant enhancement (93%) has been observed after ten cycles (see inset in Figure 3) and the discharge capacity at the end of the 60th cycle is 59 mA h g^{-1}. The observation of a constant K/V ratio of 0.45 from EDX after the 60th cycle supports the removal of one K^+ ion. A similar voltage profile, with a discharge capacity of 50 mA h g^{-1} at the end of the 30th cycle, was also observed for **1** without ball milling, but the coulombic efficiency achieved was only 72%.

The cyclic voltammogram (CV) curves of **1** (see Supporting Information, Figure S10) show the anodic (Li extraction) and cathodic (Li insertion) peak voltages at 4.18 and 3.83 V in the potential range of 2.5–4.6 V versus Li and are in agreement with the charge–discharge curves (Figure 3). These main peak voltage values corroborate the $V^{4+/5+}$ redox couple. To ascertain the electrode composition under charge and discharge states upon galvanostatic cycling, ex situ FTIR spectroscopy and PXRD experiments were carried out on several replica cells after careful dismantling and cleaning in the glove box. The ex situ FTIR spectroscopy studies on the cycled electrodes after charging show characteristic carboxylate (1645 cm^{-1}) and phosphate bands (1108 and 1064 cm^{-1}; see Supporting Information, Figure S11). This further supports the stability of **1** upon charging and discharging. The peaks at 10° and 12° correspond to (010) and (002) planes of **1** in the PXRD patterns of the charged (4.6 V) electrode after 60 cycles and exhibit the crystallinity and robustness of the framework. The calculated lattice parameters of this sample by Reitveld refinement are $a = 6.305$ Å, $b = 9.093$ Å, and $c = 14.699$ Å (see Supporting Information, Figure S12). Further complementary studies like XPS and X-ray absorption spectroscopy (XAS) techniques are needed to confirm the oxidation state and electronic structure of the above cycled electrodes. The lithium exchange experiments using **1** at room temperature shows the formation of a lithiated complex $LiK[(VO)_2(HPO_4)_2(C_2O_4)]\cdot 4.5H_2O$ (**3**). The elemental analysis shows the exchange of K^+ ions with Li^+ ions, and the PXRD pattern of the lithiated analogue **3** matches with **1** (see Supporting Information, Figure S13). This indicates the ease of exchange of K^+ ion by Li^+ ion. The electrochemical cycling curves of the chemically lithiated product, **3** and the dehydrated Na analogue $Na_2[(VO)_2(HPO_4)_2(C_2O_4)]$ (**2**) under the same conditions (Figures S14, S15) show similar voltage profiles with a discharge capacity of 55 and 60 mA h g^{-1}, respectively, at the end of the 25th cycle, where the theoretical capacity corresponding to the complete removal of alkali ions is 116 mA h g^{-1}. These results reiterate the facile extraction of alkali ions from the MOPOF. The anodic and cathodic peaks observed in the CV at 4.0 and 3.83 V correspond to the V^{IV}/V^{V} redox couple (see Supporting Information, Figure S16). Furthermore, the ex situ PXRD patterns of the bare and cycled electrodes confirm again the robustness of the material, and the EDX spectra show the removal of Na^+ ions in the first cycle (see Supporting Information, Figure S17, S18).

The reversible capacity of **1** at different C rates (0.4, 1, and 2 C) was about 68, 58, and 40 mA h g^{-1} at the end of 60 cycles, respectively. Cycling at greater than 0.6 C rate enhances the coulombic efficiency to 99% with an increase in cycling stability. The slight increase in ΔV upon increasing the C rate indicates the rapid intercalation kinetics of the MOPOF system and shows the ability of the material to achieve excellent specific storage capacity (see Supporting Information, Figure S19). Besides this, it should be mentioned that the electrochemical characteristics of the samples stored under ambient conditions for 8 months remain unchanged (see Supporting Information, Figure S20). The crystallinity, phase purity, and the sustainability in the performance of the material illustrate the chemical stability of the oxalatophosphate systems.

© 2012 Wiley-VCH Verlag GmbH & Co. KGaA, Weinheim

In summary, crystalline hybrid 4 V cathode materials with open framework structures **1**–**3** have been synthesized in gram scale. The feasibility of exchanging the K^+ with Li^+ ions was demonstrated by the isolation and characterization of the lithiated species **3**. The systematic investigation of the electrochemical performance of **1** demonstrates the facile extraction and insertion of alkali metal ions. The preliminary EIS studies of **1** and the results of the ex situ EDX spectra of **1**–**3** support that K^+ ions are extracted in the first cycle and further Li^+ ions are subsequently inserted/de-inserted. The ex situ FTIR spectra and PXRD studies of the cycled electrodes after charging at 4.6 V provided evidence for the robustness of the framework structure. Detailed structural, electrochemical, and kinetic studies will help to unravel the complexity of the ion insertion/de-insertion process as well as to improve the performance and optimization of these materials. The possibility of tailoring the system with respect to the choice of voltage and near-theoretical capacity by varying the alkali metal, transition metal, organic ligands, and polyanion moieties is expected to lead to better, cost-effective cathode materials with new architectures. Nevertheless, excellent structural features with facile migration pathways, synthetic simplicity, reversible electrochemical activity, cycling, and chemical stability of this MOPOF system pave the way for employing these materials as an alternative cathode material for commercial Li-ion cells. The MOPOF system could also be applied to the emerging field of Na-ion batteries, which is important because of the higher natural abundance of Na compared to Li.[12a,21a,23] Energy storage of the MOPOF **2** in Na-ion cells will be discussed in a forthcoming publication.

Experimental Section

1: A mixture of V_2O_5 (0.590 g, 3.24 mmol), $K_2C_2O_4$ (1.40 g, 7.6 mmol), and H_3PO_4 (4.0 mL, 60.87 mmol) in the molar ratio of 1:2.3:21, together with 10 mL of H_2O was placed in a Teflon vessel and sonicated for about 5 min. The vessel was then sealed tightly in a stainless steel autoclave and placed in the oven. It was heated to 120 °C over 1 h, maintained for 35 h, and cooled down to room temperature for 18 h. The bluish-green precipitate, **1** was washed with water and then dried under vacuum (Yield: 1.3 g, 75 %). IR (KBr): $\tilde{\nu}$ = 3162 (m), 1633 (m), 1399 (s), 1243 (w), 1100 (s), 1054 (w), 622 cm^{-1} (w). Elemental analysis calcd (%) for $C_2H_{10.5}O_{18.5}P_2K_{2.5}V_2$: C 4.05, H 1.79, P 10.46; found: C 4.15, H 1.77, P 10.22. TG under N_2 flow: calcd weight losses for $4.5{\cdot}H_2O$ and oxalate units are 13.7 and 14.9 %; found 11.8 and 14.1 %, respectively. Scaling down the reaction by tenfold with the same volume of water (10 mL) resulted in the isolation of bluish-green plate-like crystals suitable for single-crystal X-ray structure determination.

Crystal data: **1**: Triclinic space group $P\bar{1}$, $a = 6.3953(4)$, $b = 9.1451(5)$, $c = 14.6208(9)$, $\alpha = 97.269(1)$, $\beta = 91.351(1)$, $\gamma = 106.500(1)$, $V = 811.71(8)$, $Z = 2$, $\rho_{calcd} = 2.423\ g\,cm^{-3}$, $\mu = 2.088\ mm^{-1}$, $T = 223(2)$ K, $R_1 = 0.0593$, $wR_2 = 0.1680$, GOF = 1.076 for 3378 reflections with $I > 2\sigma(I)$.

Crystal data for **1** were collected on a Bruker APEX diffractometer attached with a CCD detector and graphite-monochromated $Mo_{K\alpha}$ radiation (λ, 0.71073 Å) using a sealed tube at 223(2) K. Absorption corrections were made with the program SADABS,[24] and the crystallographic package SHELXTL[25] was used for all calculations. CCDC 836146 contains the supplementary crystallographic data for this paper. These data can be obtained free of charge from The Cambridge Crystallographic Data Centre using www.ccdc.cam.ac.uk/data_request/cif.

Received: January 10, 2012
Published online: April 26, 2012

Keywords: cyclic voltammetry · electrochemistry · lithium · redox chemistry · X-ray diffraction

[1] a) F. Cheng, J. Liang, Z. Tao, J. Chen, *Adv. Mater.* **2011**, *23*, 1695 – 1715; b) Y. Wang, P. He, H. Zhou, *Energy Environ. Sci.* **2011**, *4*, 805 – 817; c) J. B. Goodenough, Y. Kim, *Chem. Mater.* **2010**, *22*, 587 – 603; d) A. Abouimrane, M. Armand, N. Ravet, *New Trends in Intercalation Compounds for Energy Storage and Conversion*, *2003 – 20. (International Symposium held 30 April-2 May 2003 in Paris, France).* (Eds.: K. Zaghib, C. M. Julien, J. Prakash), *The Electrochemical Society, Inc, Pennington, USA*, **2003**, pp. 15 – 22.

[2] A. K. Padhi, K. S. Nanjundaswamy, J. B. Goodenough, *J. Electrochem. Soc.* **1997**, *144*, 1188 – 1194.

[3] a) C. Delacourt, P. Poizot, S. Levasseur, C. Masquelier, *Electrochem. Solid-State Lett.* **2006**, *9*, A352 – A355; b) K. Saravanan, M. V. Reddy, P. Balaya, H. Gong, B. V. R. Chowdari, J. J. Vittal, *J. Mater. Chem.* **2009**, *19*, 605 – 610.

[4] a) P. S. Herle, B. Ellis, N. Coombs, L. F. Nazar, *Nat. Mater.* **2004**, *3*, 147 – 152; b) D. Lepage, C. Michot, G. Liang, M. Gauthier, S. B. Schougaard, *Angew. Chem.* **2011**, *123*, 7016 – 7019; *Angew. Chem. Int. Ed.* **2011**, *50*, 6884 – 6887; c) J. Wang, X. Sun, *Energy Environ. Sci.* **2012**, *5*, 5163 – 5185.

[5] S.-Y. Chung, J. T. Bloking, Y.-M. Chiang, *Nat. Mater.* **2002**, *1*, 123 – 128.

[6] a) C. Sun, S. Rajasekhara, J. B. Goodenough, F. Zhou, *J. Am. Chem. Soc.* **2011**, *133*, 2132 – 2135; b) C. Zhu, Y. Yu, L. Gu, K. Weichert, J. Maier, *Angew. Chem.* **2011**, *123*, 6402 – 6406; *Angew. Chem. Int. Ed.* **2011**, *50*, 6278 – 6282.

[7] C. Masquelier, C. Wurm, J. Rodríguez-Carvajal, J. Gaubicher, L. Nazar, *Chem. Mater.* **2000**, *12*, 525 – 532.

[8] a) N. Kuganathan, M. S. Islam, *Chem. Mater.* **2009**, *21*, 5196 – 5202; b) S.-I. Nishimura, S. Hayase, R. Kanno, M. Yashima, N. Nakayama, A. Yamada, *J. Am. Chem. Soc.* **2008**, *130*, 13212 – 13213.

[9] a) A. S. Aricò, P. Bruce, B. Scrosati, J.-M. Tarascon, W. van Schalkwijk, *Nat. Mater.* **2005**, *4*, 366 – 377; b) P. Barpanda, M. Ati, B. C. Melot, G. Rousse, J. N. Chotard, M. L. Doublet, M. T. Sougrati, S. A. Corr, J. C. Jumas, J. M. Tarascon, *Nat. Mater.* **2011**, *10*, 772 – 779.

[10] A. Yamada, N. Iwane, Y. Harada, S.-I. Nishimura, Y. Koyama, I. Tanaka, *Adv. Mater.* **2010**, *22*, 3583 – 3587.

[11] a) T. A. Kerr, J. Gaubicher, L. F. Nazar, *Electrochem. Solid-State Lett.* **2000**, *3*, 460 – 462; b) K. Saravanan, H. S. Lee, M. Kuezma, J. J. Vittal, P. Balaya, *J. Mater. Chem.* **2011**, *21*, 10042 – 10050.

[12] a) J. Barker, M. Y. Saidi, J. L. Swoyer, *J. Electrochem. Soc.* **2004**, *151*, A1670 – A1677; b) M. V. Reddy, G. V. Subba Rao, B. V. R. Chowdari, *J. Power Sources* **2010**, *195*, 5768 – 5774.

[13] S.-I. Nishimura, M. Nakamura, R. Natsui, A. Yamada, *J. Am. Chem. Soc.* **2010**, *132*, 13596 – 13597.

[14] a) P. Poizot, F. Dolhem, *Energy Environ. Sci.* **2011**, *4*, 2003 – 2019; b) Y. Morita, S. Nishida, T. Murata, M. Moriguchi, A. Ueda, M. Satoh, K. Arifuku, K. Sato, T. Takui, *Nat. Mater.* **2011**, *10*, 947 – 951; c) S. Renault, J. Geng, F. Dolhem, P. Poizot, *Chem. Commun.* **2011**, *47*, 2414 – 2416.

[15] a) G. Férey, F. Millange, M. Morcrette, C. Serre, M.-L. Doublet, J.-M. Grenèche, J.-M. Tarascon, *Angew. Chem.* **2007**, *119*, 3323 – 3327; *Angew. Chem. Int. Ed.* **2007**, *46*, 3259 – 3263; b) G. de Combarieu, M. Morcrette, F. Millange, N. Guillou, J. Cabana, C. P. Grey, I. Margiolaki, G. Fe'rey, J. M. Tarascon, *Chem. Mater.* **2009**, *21*, 1602 – 1611; c) K. Saravanan, M.

 © 2012 Wiley-VCH Verlag GmbH & Co. KGaA, Weinheim

Nagarathinam, P. Balaya, J. J. Vittal, *J. Mater. Chem.* **2010**, *20*, 8329 – 8335; d) M. Okubo, D. Asakura, Y. Mizuno, T. Kudo, H. Zhou, A. Okazawa, N. Kojima, K. Ikedo, T. Mizokawa, I. Honma, *Angew. Chem.* **2011**, *123*, 6393 – 6397; *Angew. Chem. Int. Ed.* **2011**, *50*, 6269 – 6273; e) T. L. A. Nguyen, R. Demir-Cakan, T. Devic, M. Morcrette, T. Ahnfeldt, P. Auban-Senzier, N. Stock, A.-M. Goncalves, Y. Filinchuk, J.-M. Tarascon, G. Fe'rey, *Inorg. Chem.* **2010**, *49*, 7135 – 7143.

[16] a) S. Natarajan, S. Mandal, *Angew. Chem.* **2008**, *120*, 4876 – 4907; *Angew. Chem. Int. Ed.* **2008**, *47*, 4798 – 4828; b) C.-Y. Sheu, S.-F. Lee, K.-H. Lii, *Inorg. Chem.* **2006**, *45*, 1891 – 1893.

[17] a) F. R. Kizewski, P. Boyle, D. Hesterberg, J. D. Martin, *J. Am. Chem. Soc.* **2010**, *132*, 2301 – 2308; b) Y.-C. Yang, S.-L. Wang, *J. Am. Chem. Soc.* **2008**, *130*, 1146 – 1147; c) S.-H. Huang, C.-H. Lin, W.-C. Wu, S.-L. Wang, *Angew. Chem.* **2009**, *121*, 6240 – 6243; *Angew. Chem. Int. Ed.* **2009**, *48*, 6124 – 6127.

[18] a) I. D. Brown, D. Altermatt, *Acta Crystallogr. Sect. B* **1985**, *41*, 244 – 247; b) M. Schindler, F. C. Hawthorne, W. H. Baur, *Chem. Mater.* **2000**, *12*, 1248 – 1259; c) M. B. Robin, P. Day in *Adv. Inorg. Chem. Vol. 10* (Eds.: H. J. Emeléus, A. G. Sharpe), Academic Press, New York, **1968**, pp. 247 – 422.

[19] C. A. J. Fisher, V. M. Hart Prieto, M. S. Islam, *Chem. Mater.* **2008**, *20*, 5907 – 5915.

[20] J. F. Colin, T. Bataille, S. E. Ashbrook, N. Audebrand, L. Le Pollès, J. Y. Pivan, E. Le Fur, *Inorg. Chem.* **2006**, *45*, 6034 – 6040.

[21] a) R. Tripathi, G. R. Gardiner, M. S. Islam, L. F. Nazar, *Chem. Mater.* **2011**, *23*, 2278 – 2284; b) B. L. Ellis, W. R. M. Makahnouk, Y. Makimura, K. Toghill, L. F. Nazar, *Nat. Mater.* **2007**, *6*, 749 – 753.

[22] a) Z. Bakenov, I. Taniguchi, *J. Electrochem. Soc.* **2010**, *157*, A430 – A436; b) M. Konarova, I. Taniguchi, *J. Power Sources* **2009**, *194*, 1029 – 1035.

[23] R. Tripathi, T. N. Ramesh, B. L. Ellis, L. F. Nazar, *Angew. Chem.* **2010**, *122*, 8920 – 8924; *Angew. Chem. Int. Ed.* **2010**, *49*, 8738 – 8742.

[24] G. M. Sheldrick, SADABS, Program for Empirical Absorption Correction for Area Detector Data; University of Göttingen: Göttingen, Germany, **2000**.

[25] SHELXTL Reference Manual, Version 5.1; Bruker AXS, Analytical X-ray Systems, Inc.: Madison, WI, **1997**.

 © 2012 Wiley-VCH Verlag GmbH & Co. KGaA, Weinheim